GeoArabia, Vol. 1, No. 2, 1996
Gulf PetroLink, Bahrain

Geostatistical Model for the Arab-D Reservoir, North 'Ain Dar Pilot, Ghawar Field, Saudi Arabia: An Improved Reservoir Simulation Model

John L. Douglas and Members of the 'Ain Dar/Shedgum Modeling Team
Saudi Aramco

ABSTRACT

The North 'Ain Dar 3-D geocellular model consists of geostatistical models for electrofacies, porosity and permeability for a portion of the Jurassic Arab-D reservoir of Ghawar field, Saudi Arabia. The reservoir consists of a series of shallow water carbonate shelf sediments and is subdivided into 10 time-stratigraphic slices on the basis of core descriptions and gamma/porosity log correlations. The North 'Ain Dar model includes an electrofacies model and electrofacies-dependent porosity and permeability models. *Sequential Indicator Simulations* were used to create the electrofacies and porosity models. *Cloud Transform Simulations* were used to generate permeability models. Advantages of the geostatistical modeling approach used here include: (1) porosity and permeability models are constrained by the electrofacies model, i.e. by the distribution of reservoir rock types; (2) patterns of spatial correlation and variability present in well log and core data are built into the models; (3) data extremes are preserved and are incorporated into the model. These are critical when it comes to determining fluid flow patterns in the reservoir.

Comparison of model Kh with production data Kh indicates that the stratigraphic boundaries used in the model generally coincide with shifts in fluid flow as indicated by flowmeter data, and therefore represent reasonable flow unit boundaries. Further, model permeability and production estimated permeability are correlated on a Kh basis, in terms of vertical patterns of distribution and cumulative Kh values at well locations. This agreement between model and well test Kh improves on previous, deterministic models of the Arab-D reservoir and indicates that the modeling approach used in North 'Ain Dar should be applicable to other portions of the Ghawar reservoir.

INTRODUCTION

The North 'Ain Dar Pilot covers an area of 25 by 25 kilometers (km) and is situated at the northern end of Ghawar field, in the Eastern Province of Saudi Arabia (Figure 1). The pilot is one of a series of models currently being generated of the Arab-D reservoir in the northern, 'Ain Dar and Shedgum area, of Ghawar field. The models will be used in simulation studies, and should, therefore, capture the major reservoir flow units that are present in the reservoir.

The field is being exploited by means of a peripheral water injection scheme, with injectors providing support to producers situated on the crest of the structure (see Figure 1 for well type disposition). Critical factors bearing on the success of any reservoir description model are the spatial distribution within the model of extreme values in porosity and permeability, as these will in large measure determine the pathways of fluid flow in the reservoir. Historically, one of the major problems in this portion of the 'Ain Dar reservoir has been the irregular advance of the waterflood front from the injectors toward the producers, especially on the shallower-dipping eastern flank of the structure (see Figure 1); the previous, deterministic simulation model covering this part of the reservoir has been unable to replicate the embayments and protrusions of the flood front indicated by production data.

This paper will focus on reviewing the geostatistical model that was built, and, in particular, on the utility of the model as it is presently known. The geological setting of the Arab-D reservoir and descriptions of the geostatistical methods used to create the model will be dealt with in summary fashion only.

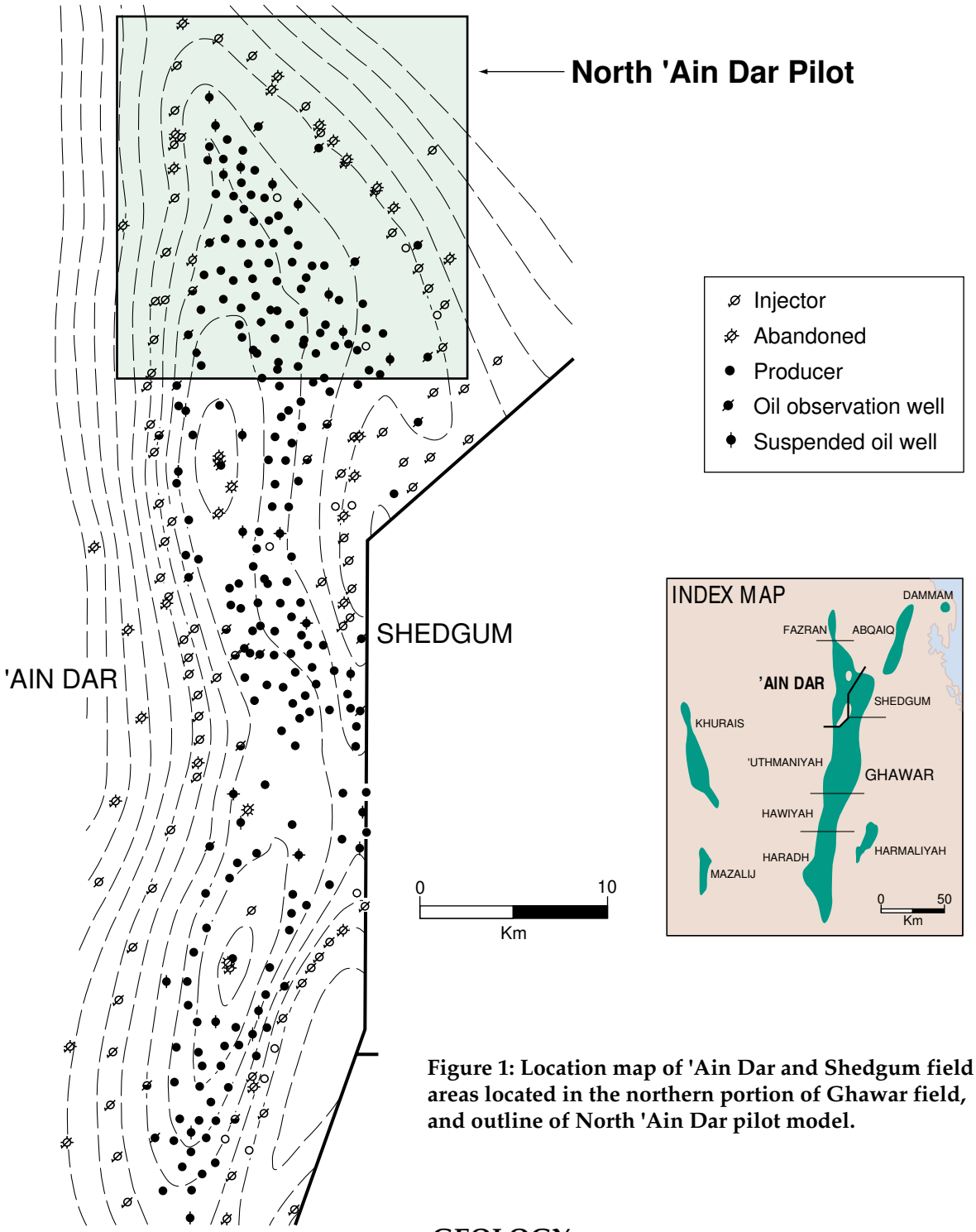

Figure 1: Location map of 'Ain Dar and Shedgum field areas located in the northern portion of Ghawar field, and outline of North 'Ain Dar pilot model.

GEOLOGY

Geologic Setting

The Arab-D reservoir is comprised of a series of shallow water, platformal carbonate sediments. In the study area, these sediments form overall a cleaning-up and a shallowing-up succession. The bulk of the reservoir is comprised of limestone, though some dolomite is present. Anhydrite is present, but in minor amounts only. The cleanest and most porous rocks - hence the most favorable from a production point of view - are situated in the upper portion of the reservoir. Interparticle porosity predominates in the reservoir, though locally, other porosity types are important; for example, moldic and intercrystalline porosity in dolomitized portions of the reservoir.

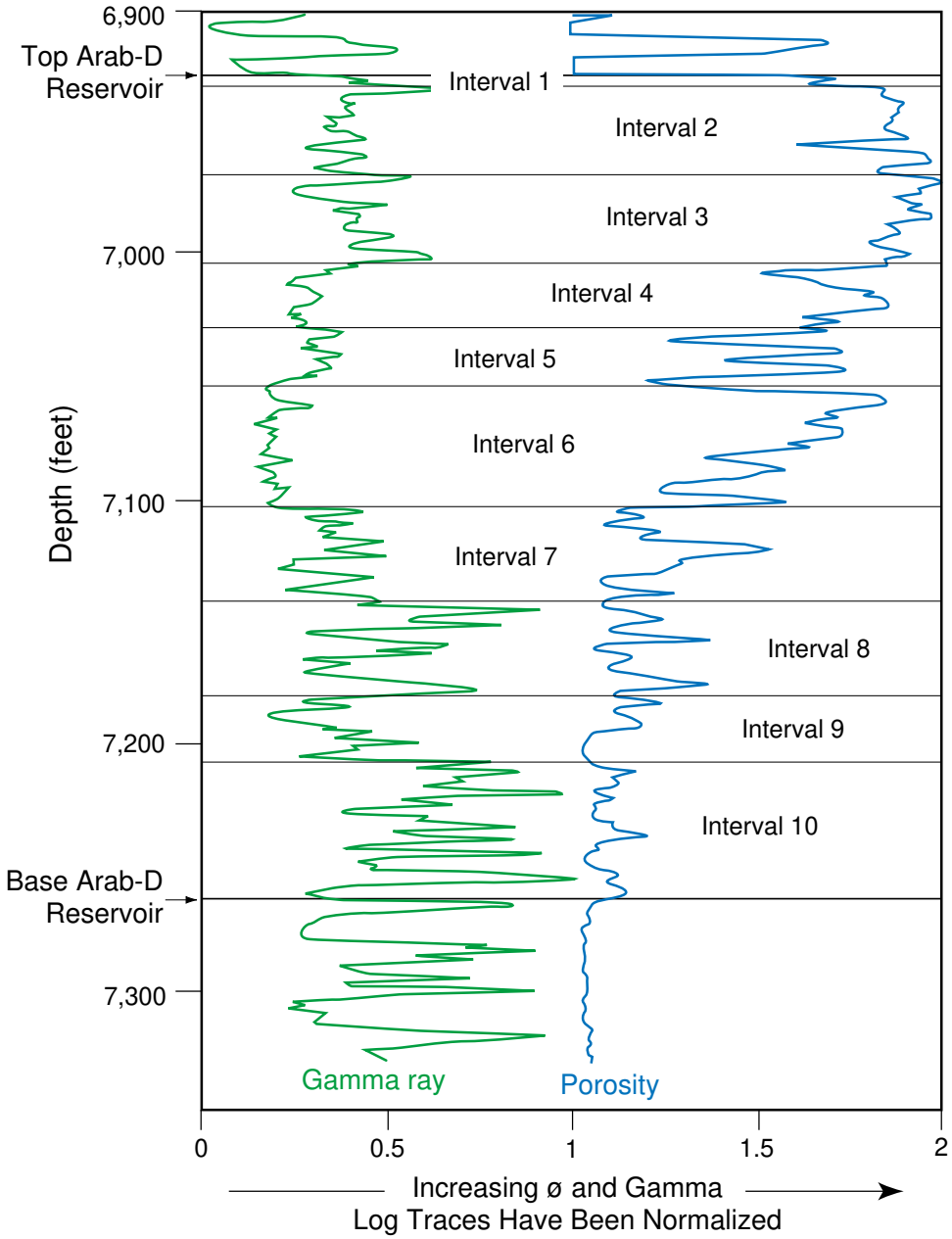

Figure 2: Type log showing stratigraphic framework for North 'Ain Dar pilot area as defined by a combination of porosity and gamma ray logs.

Stratigraphic Framework

Well log correlation of porosity and gamma ray traces, in conjunction with the information obtained from petrographic core descriptions, have been used to develop a stratigraphic framework for the model area. Eleven marker surfaces, defining ten reservoir intervals, were determined by the porosity and gamma log traces (Figure 2). The lower portion of the reservoir (Intervals 8-10) is characterized by strong cyclicity, by relatively high gamma counts and relatively low porosity. The cycles in this lower, mud-rich portion of the reservoir are highly correlatable and exhibit little character change over the pilot area. Data from available core descriptions from North 'Ain Dar and adjacent areas suggest a shallow water depositional environment (Bova, 1994). Cycle tops are commonly sharply defined by hardground surfaces upon which detrital silicates are present; de-dolomite is sometimes developed in the vicinity of the cycle boundaries. These features suggest that this portion of the reservoir may have been subjected to occasional subaerial exposure (Bova, 1994).

The central portion of the reservoir (Intervals 6-7) is characterized by a stepwise cleaning-up of the gamma log trace, and a greater development of porosity, in somewhat thicker cycles. The upward cleaning-up of the gamma ray trace is accompanied by a gradual reduction in the proportion of lime mud in the depositional system. The proportion of grain supported textures is accordingly greater than in the underlying basal section of the reservoir.

In reservoir Interval 5, the presence of an open marine faunal assemblage characterized by stromatoporoids and corals reflects an open marine depositional environment. Mud supported textures are predominant in this interval, suggesting that deposition occurred at or below wave base. The available petrographic data indicates that this is probably the deepest water portion of the Arab-D reservoir in the North 'Ain Dar area. The muddy depositional fabrics in this interval are more susceptible to dolomitization than rocks in the bounding reservoir intervals, and consequently the interval has been dolomitized to a greater extent.

Above Interval 5, grain-supported carbonate sediments, including local oolitic grainstones, are predominant. Core data indicates that this portion of the reservoir is characterized by the highest porosity and permeability, making it the most important from a reservoir production perspective. Available core descriptions suggest that environmentally this portion of the reservoir forms a shallowing-up sequence. Interval 1 forms the top of the reservoir, locally contains tidal flat textures, is commonly dolomitized, and grades upwards into the anhydrite which forms the seal to the reservoir.

The ten reservoir intervals discussed above are believed to represent chronostratigraphic slices in the reservoir. The thicker intervals in the lower portion of the model (e.g. below Interval 6 on Figure 3) could readily have been subdivided into thinner time slices; this was not done because the lower, tight portion of the reservoir contributes very little to fluid movement and to production in the study area. All 10 stratigraphic slices were in any event subdivided proportionally into finer slices during modeling operations.

ADVANTAGES OF A GEOSTATISTICAL MODELING APPROACH

Geostatistical modeling methods were used to create the North 'Ain Dar model. A geostatistical approach, versus a deterministic approach, was adopted in view of the potential advantages offered by geostatistical modeling. These advantages include:

(1) A model in which the distribution of porosity and permeability are constrained by the distribution of the constituent rock types (electrofacies) contained in the model.

(2) The incorporation of patterns of spatial correlation developed from core and well log data for fundamental attributes of interest (rock types, porosity, permeability) that are used to build the model.

(3) The preservation of the full range of data variability, including extreme values, of porosity and permeability as defined by the available core plug data. The inclusion of data extremes in the model is of particular importance as the spatial distribution of extremes values plays an important role in shaping the patterns of fluid flow in the reservoir.

Several of these advantages are illustrated in Figure 3, a comparison of two porosity models for one of the 10 stratigraphic slices. On the top, is the average porosity of the interval as produced by a deterministic (inverse weighted distance) modeling approach, while on the bottom is the equivalent geostatistical model (Sequential Indicator Simulation) for the same input well log porosity data. It is evident that there is considerably more spatial 'character' or variability in the geostatistical model, and that the deterministic model is noticeably smoother (Figure 3).

The spatial 'character' seen in the geostatistical model is not noise, but rather reflects the spatial structure of the input well porosity data as determined by variogram analysis. Note also that these patterns are present throughout the entire model, including areas that lie outside of the available well control. The deterministic model, in contrast, is noticeably smoother outside the limits of the well control (Figure 3).

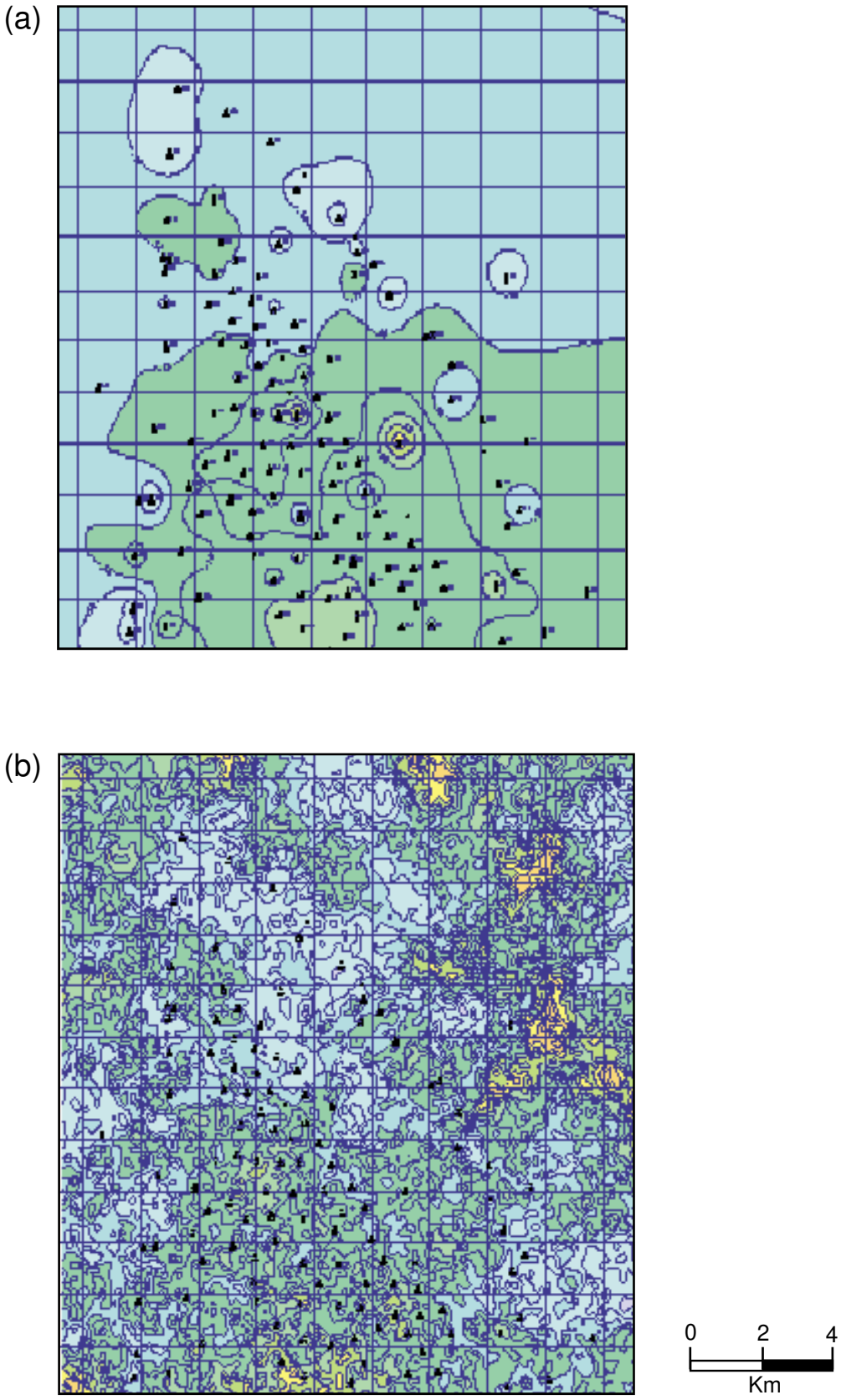

Figure 3: Comparison of (a) deterministic porosity modeling inverse weighted distance versus (b) geostatistical porosity modeling Sequential Indicator Simulation (SIS) for same stratigraphic interval. Warmer colors represent higher porosity.

GEOSTATISTICAL MODELING METHODOLOGY

The composite geostatistical model of the North 'Ain Dar Arab-D reservoir was constructed as follows:

Stratigraphic Framework

A sequence stratigraphic model was constructed, as described previously. The ten reservoir intervals defined in this way served as the framework for the geocellular model in which all subsequent work was done. The correlation marker surfaces defining the 10 stratigraphic slices were mapped in Z-MapPlus and imported directly into the Geolith and Stratamodel applications used to generate the geostatistical models (see below).

Geocellular Modeling

The marker surfaces mapped out during the course of putting together the stratigraphic model were then used to construct a geocellular framework. The pilot itself measured 25 by 25 kilometers, and was gridded using a cell size of 250 by 250 meters. The ten reservoir intervals defined by the stratigraphic framework were further divided, for modeling purposes, into a total of 210 proportional layers, each on average 1.5 feet thick. The resulting model cube contains a total of 2.1 million cells.

Electrofacies in Cored Wells

Available core-plug porosity and permeability data together with petrographic attribute data from the same plugs was then analyzed to determine which rock groupings were most distinct in terms of the porosity and permeability populations represented. These groupings were then used to define electrofacies, based on the relationship between the rock groups and the open hole log suite. In all, four electrofacies were used in modeling: dolomite, undifferentiated limestone, grainstone, and packstone. Figure 4 shows the distinct porosity and permeability fields occupied by two electrofacies, grainstone and packstone, for two wells in the pilot for which core-derived rock-fabric data was available over the entire cored interval. The grainstones occur in the high porosity and high permeability portion of the scatterplot, whereas the muddier, packstone electrofacies falls along a lower porosity and permeability trend (Figure 4). Ideally, it would be desirable to further subdivide the Dunham classification based

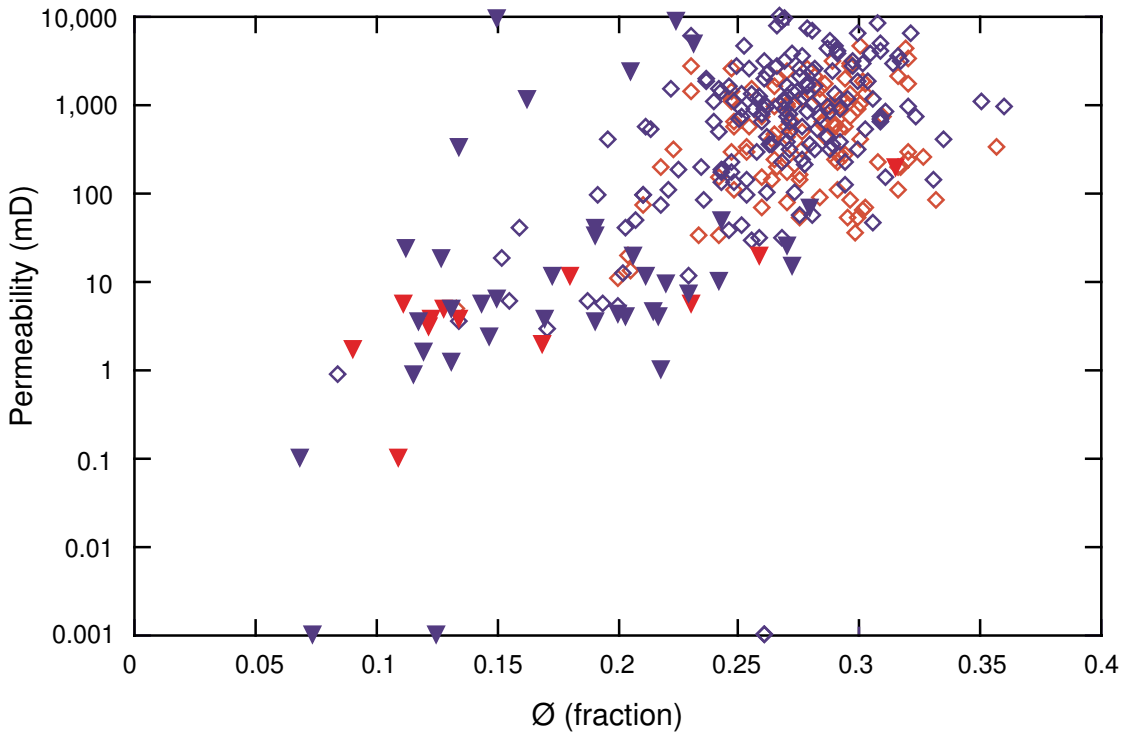

Figure 4: Relationship between porosity and permeability for specific rock-fabric units from two North 'Ain Dar cores. Note that grainstones and mud-lean packstones (open diamonds) plot in a distinct porosity-permeability field relative to packstones, wackestones, and mudstones (solid triangles). Core plug data from upper third of reservoir; dolomite plugs have been excluded.

electrofacies shown in Figure 4, in view of the considerable 'scatter' present in the porosity and permeability field each represents. This was not possible with the data available at the time the North 'Ain Dar models were generated.

Prediction of Electrofacies in Uncored Wells

The open hole log suite was used to predict electrofacies in uncored wells. Limestone and dolomite (≥75% computed mineral dolomite) predictions were made using a series of algorithms involving the neutron, bulk density and sonic logs, as well as the log computed porosity and saturation log traces. Where these logs were not available, dolomite was 'hand-picked' using the available porosity and resistivity logs. Low porosity, high resistivity intervals correlatable with dolomites in offset wells were classified as dolomite in this way. Grainstone and packstone electrofacies were split out of limestone portions of the reservoir using the open log suite by means of a discriminate function analysis in which the 'hard' petrographic data from described cores served as a training data set.

The limestone, dolomite, grainstone and packstone well log traces generated in this way were used to create geostatistical models of electrofacies, porosity and permeability. It should be noted that the process was tailored to fit the reservoir. For example, in the lower portion of the reservoir (Intervals 8-10 on Figure 2), the grainstone electrofacies was volumetrically insignificant and a single limestone electrofacies was used.

Creation of Geostatistical Models

The electrofacies traces generated as described above were then used to create a series of geostatistical models. Chevron's GEOLITH application (version 9407) was used for this purpose. Stratigraphic framework grids created in Z-MapPlus were imported directly into Geolith and used *unchanged* as marker surfaces during modeling work. All attribute models built were three-dimensional and based on horizontal and vertical variogram models created in Geolith. Isotropic variogram models were employed throughout, as initial test work with directional variogram models did not detect any appreciable bias in indicator facies or porosity data within the study area. This lack of bias is consistent with available well data. For example, in the case of porosity data, the two wells situated furthest down-structure (see Figure 1) contain as much porosity in the upper, most critical third of the reservoir as do producing wells on the structural crest. There are no indications of a structurally controlled decrease in porosity on the flanks of the reservoir in this portion of the Ghawar structure. For generating electrofacies and

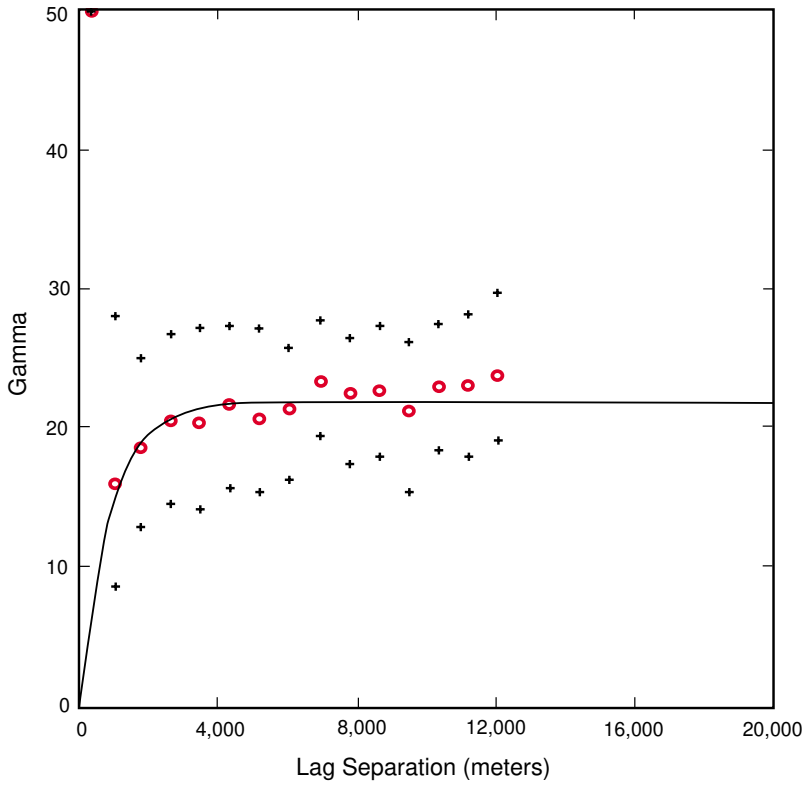

Figure 5: North 'Ain Dar isotropic horizontal indicator variogram for packstone electrofacies - model interval 7. Exponential model range 2,650, sill 0.93. Red circles indicate average gamma for all proportional layers in interval; small crosses indicate maximum and minimum gamma of proportional layers.

electrofacies specific porosity models, a Sequential Indicator Simulation (SIS) approach was adopted (see Srivastiva, 1994a). A Cloud Transform approach was used to generate electrofacies specific porosity models; probability or 'p' fields generated from electrofacies specific porosity variogram models were applied to the cloud transforms to minimize the juxtaposing of extreme high and low values (see Bashore, 1994; Srivastiva, 1994a,b). Examples of the variogram models used to generate the geostatistical models under discussion are shown in Figures 5, 6 and 7. Exponential variogram models were used throughout most of the modeling, as shown, except for the two lowest stratigraphic slices in the reservoir, where spherical models were employed.

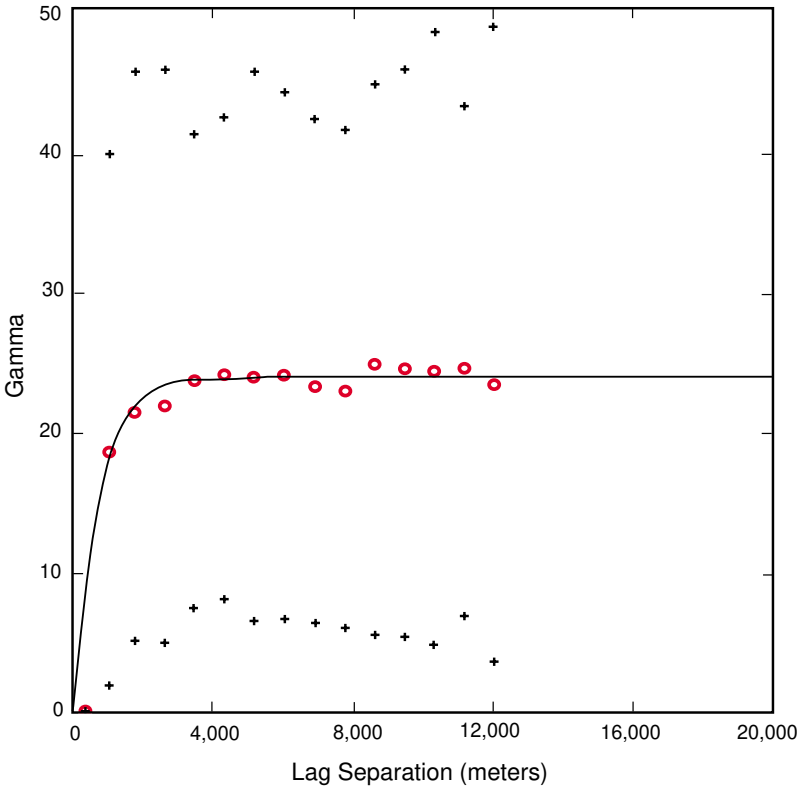

Figure 6: North 'Ain Dar isotropic horizontal porosity variogram model for packstone electrofacies - model interval 7. Exponential model range 2,137, sill 1.00. Red circles indicate average gamma for lag of all proportional layers in interval; small crosses indicate maximum and minimum gamma for proportional layers.

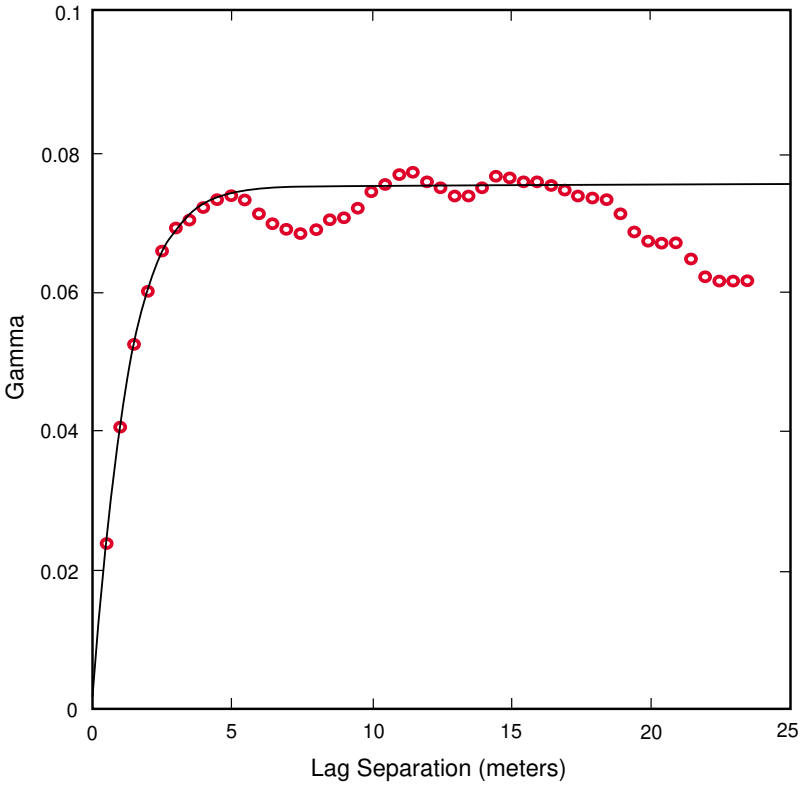

Figure 7: North 'Ain Dar isotropic vertical variogram model for porosity for packstone electrofacies - model interval 7. Exponential model range 3.63, sill 49.9. Red circles indicate gamma value for given lag separation.

The geostatistical models for electrofacies, porosity and permeability used to create composite models for the whole reservoir were built in the following order:

(a) electrofacies models (limestone/dolomite, then dolomite/grainstone/packstone);
(b) electrofacies specific porosity models; and
(c) electrofacies specific permeability models.

Separate models were generated for each of the ten reservoir intervals; these models were then appended to form single models covering the entire reservoir. Finally, composite geocellular models were created in Stratamodel by using the electrofacies indicator attribute as a flag to select the appropriate facies specific porosity and permeability values.

A total of five realizations for porosity and permeability were created; one of these is currently in the process of being simulated. Comparison of the output geostatistical models with 'hard' input data shows that the models honor the hard data.

Table 1 compares input and output data for electrofacies models in reservoir Interval 3.

Table 1
Comparison of Electrofacies Proportions in Interval 3

Input 'Facies' Data	Realization 1	Realization 2	Realization 3	Realization 4	Realization 5
Dolomite (15.8%)	17.5%	15.4%	16.2%	13.5%	14.8%
Packstone (48.1%)	49.9%	49.4%	49.7%	49.3%	49.5%
Grainstone (36.0%)	32.5%	35.1%	34.0%	37.2%	35.6%

Table 2 compares facies specific porosity and permeability data from four realizations to average porosity and permeability for the electrofacies as measured by the available core plug data. Data covers reservoir interval 3.

Table 2
Comparison of Porosity and Permeability

Core Plug Average	Realization 1	Realization 2	Realization 3	Realization 4
Dolomite ø (16.6%)	17.5%	16.5%	16.2%	17.7%
Dolomite K (207 md)	137 md	155 md	186 md	182 md
Packstone ø (22.9%)	20.7%	20.2%	19.9%	20.5%
Packstone K (438 md)	379 md	353 md	341 md	368 md
Grainstone ø (26.8%)	25.9%	25.9%	25.7%	26.3%
Grainstone K (884 md)	755 md	751 md	725 md	762 md

Note: ø represents percent porosity and K represents permeability in md.

The models also honor data at well locations, though the match is complicated in the case of core plug data by layer averaging (model layers, on average, are approximately 1.5 feet thick, whereas core plug data is reported on a 0.5 foot sample basis. Each model layer contains as many as three core plug data points). Figure 8 compares model, well log and core plug porosity at one of the well locations in the study area. Model and log porosity track closely, as they should, given that the models were built using well log porosity. The core plug data, shown in brown on Figure 8, does not match the model as closely. In part, this results from the averaging effect referred to above; the greater absolute variability in the core plug data probably reflects the smaller sample volume represented, relative to the well log data.

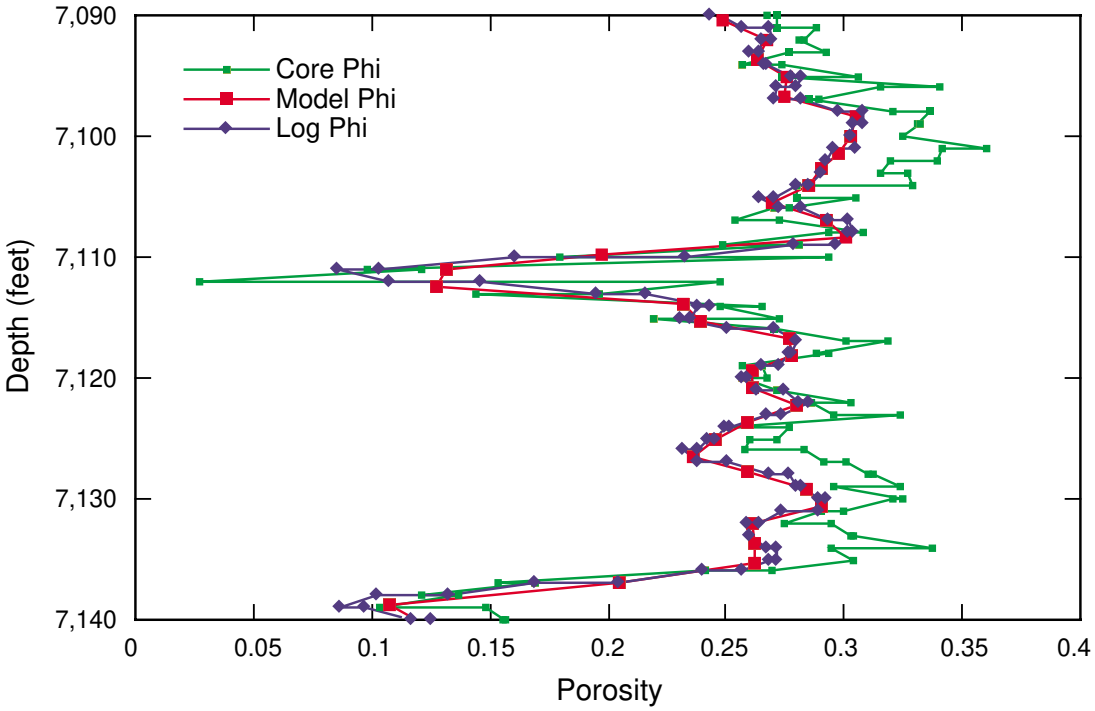

Figure 8: Comparison of core plug, model and well log porosity data in cored well in pilot.

DISCUSSION AND RESULTS

Examination of the geological models produced for the North 'Ain Dar pilot suggest that the final, composite model is a significantly useful one for simulation, forecasting and reservoir management. The electrofacies model is consistent with what is known about the reservoir where core is available. The porosity and permeability distributions in the various electrofacies specific porosity and permeability models are those one would expect from the 'hard' core plug data. The model, significantly, is highly correlated with permeability estimates obtained independently from engineering well tests. Examples of these relationships are briefly described in the remainder of this section.

Electrofacies Model

An example of the electrofacies model is shown in Figure 9. The model is consistent with what is known about the reservoir from petrographic core descriptions. For example, Interval 5, with its deeper water, muddier sediments, is preferentially dolomitized to a greater degree than the intervals above and below it, as it is based on core descriptions. Similarly, the majority of the grainstone electrofacies is developed toward the top of the reservoir in Intervals 3 and 4, and this too is compatible with the core descriptions in the pilot area.

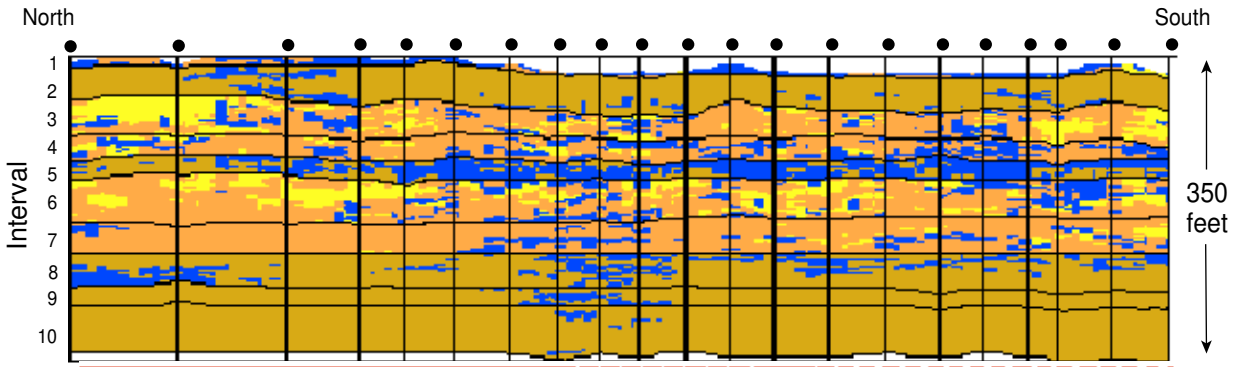

Figure 9: A north-south cross-section of the electrofacies model through the entire pilot study area. Yellow denotes 'grainstone' electrofacies, orange 'packstone', brown 'undifferentiated limestone' and blue 'dolomite'.

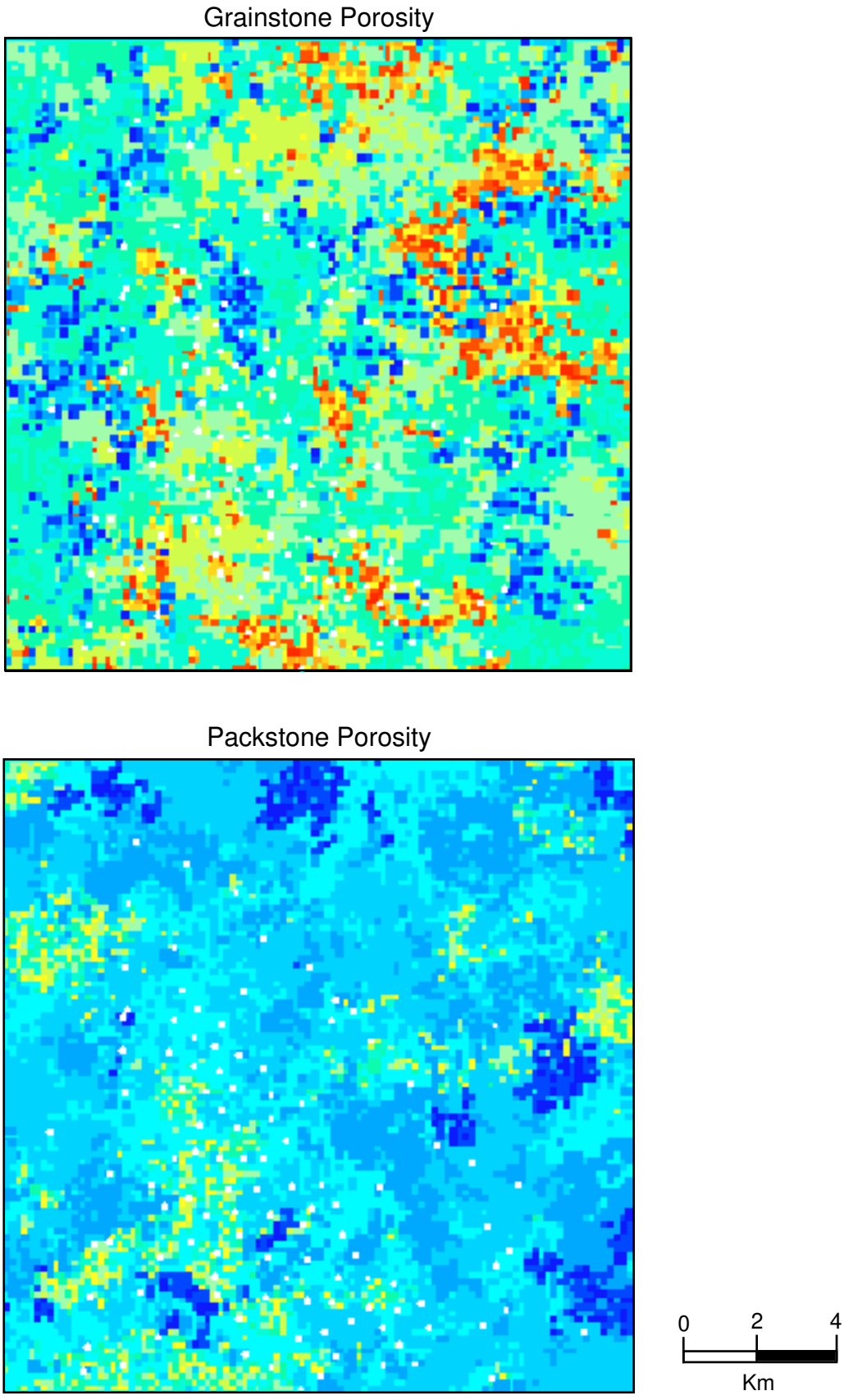

Figure 10: Comparison of SIS porosity models from the same stratigraphic interval for two different electrofacies, grainstone on the top and packstone on the bottom. Warmer colors represent higher porosity. The presence of abundant lime mud within the interparticle pore spaces of the packstones is reflected in the porosity modeling.

Electrofacies Specific Porosity Models

The electrofacies represent different porosity and permeability fields (Figure 4), which is reflected in the porosity models generated for each individual electrofacies. The porosity models for grainstone and packstone for one of the 210 reservoir layers are shown in Figure 10. This layer, regionally, is an admixture of grainstone and packstone facies, but as would be expected, the grainstone porosity model contains considerably more high porosity than the packstone model (Figure 10).

Electrofacies Specific Permeability Models

The cloud transform method used to model facies specific permeability preserves the full range of variability of input core plug porosity and permeability data. This can be seen in Figure 11, where at the top is a porosity and permeability scatterplot for packstone electrofacies core plugs in Interval 3, while at the bottom, there is a scatterplot of porosity and permeability data from the resulting model. The 'before' and 'after' scatterplots of 'hard' (core plug) data versus model input data, respectively, are equivalent. Of equal importance is that the extremes of the data have been preserved and incorporated into the model.

The permeability models for different electrofacies should also reflect the distinct porosity and permeability populations represented by the electrofacies. This is indeed the case, as is apparent in Figure 12, a comparison of grainstone and packstone electrofacies permeabilities for one of the proportional slices in Interval 6. The grainstone permeabilities are considerably higher than the corresponding packstone values, as would be expected.

Figure 13 compares the facies specific porosity and permeability models for the packstone electrofacies for one of the proportional layers in Interval 6. Spatially, the models are correlated, as should be the case, given the correlation developed between porosity and permeability in the 'hard' data scatterplot shown in Figure 11.

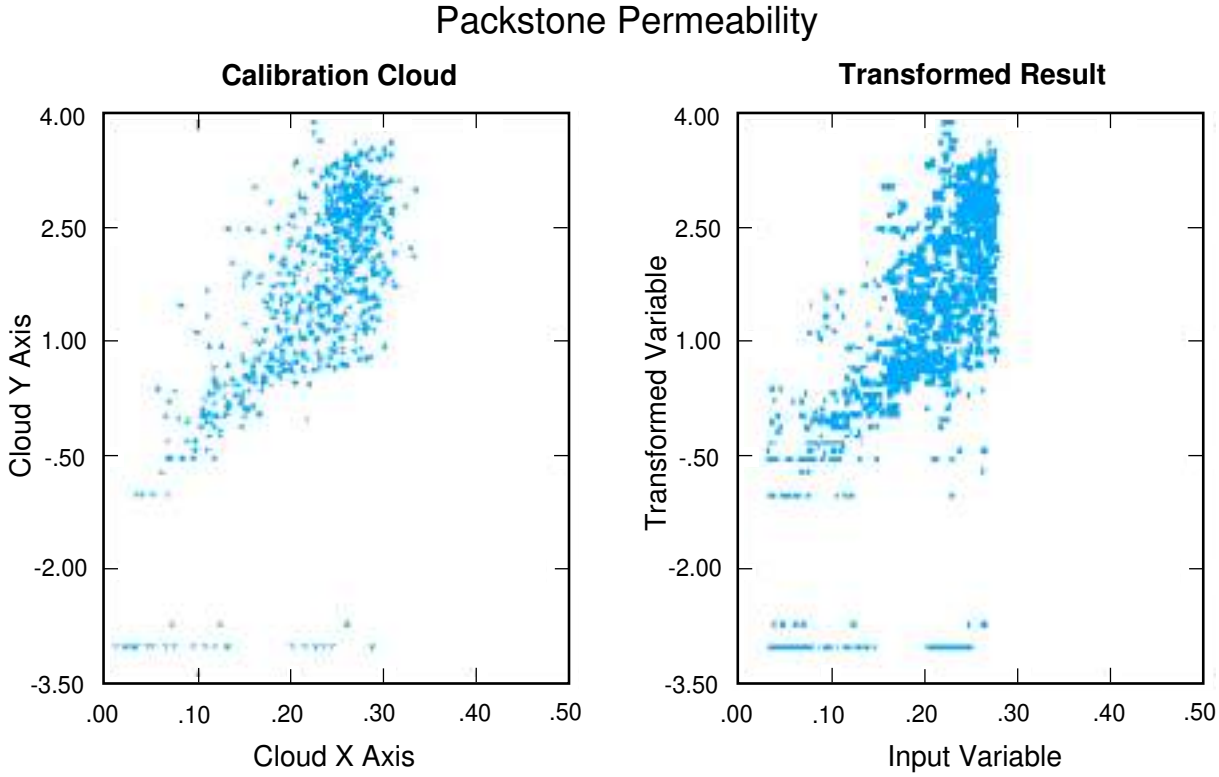

Figure 11: Cloud transform model comparing the raw input data from core plugs (left cloud) with the output transformed result (right cloud). The data is for one electrofacies (packstone) within a single stratigraphic interval. Note that the cloud transform replicates the variability or 'shape' of the input core plug data. Note in particular that the low permeability 'tail' visible in the core plug data is also present in the model.

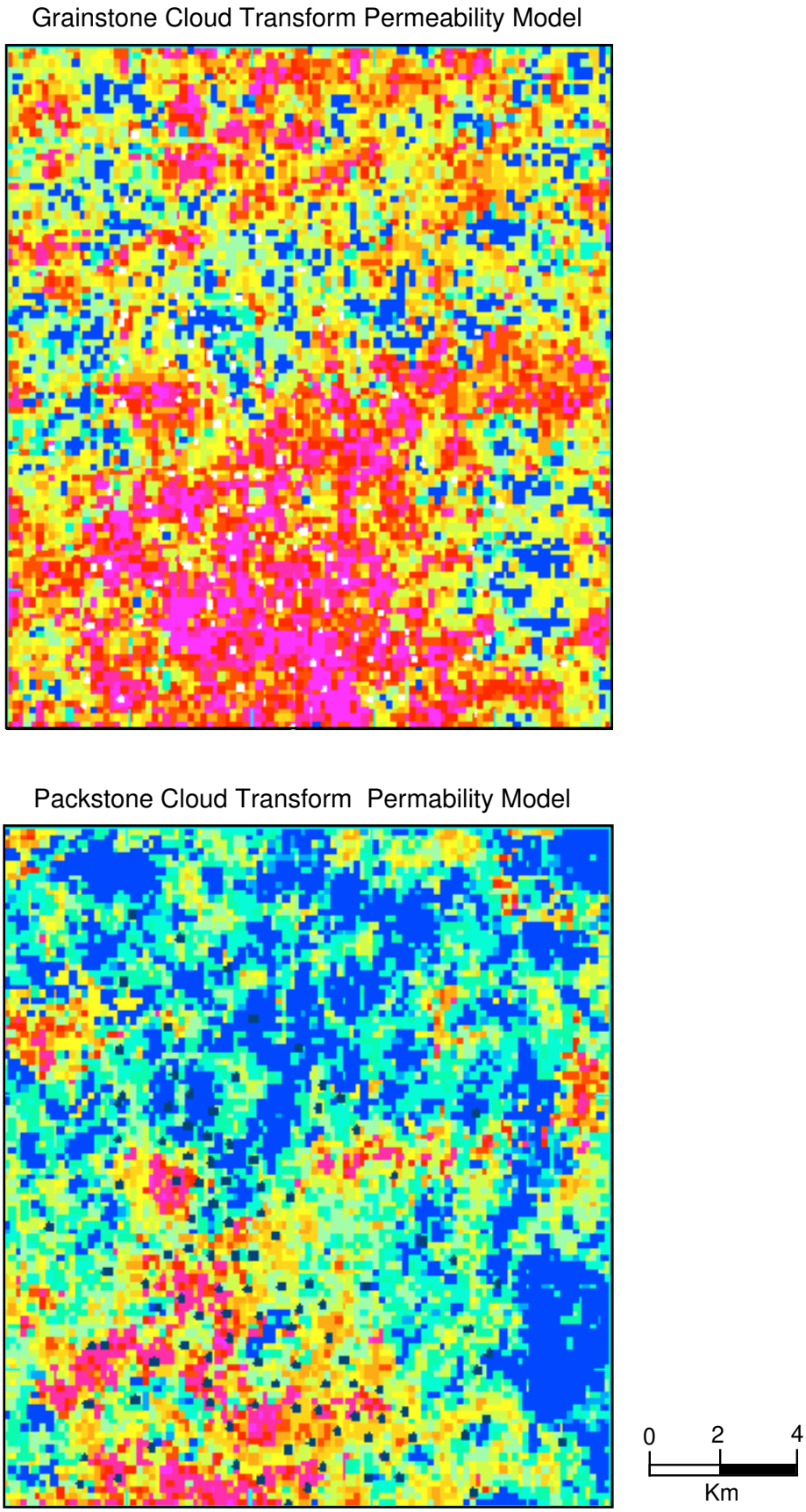

Figure 12: Comparison of cloud transform permeability models for two constrasting electrofacies, grainstone (top) and packstone (bottom). As was noticed in the porosity modeling, the packstones show much lower permeability. Warmer colors represent higher permeability.

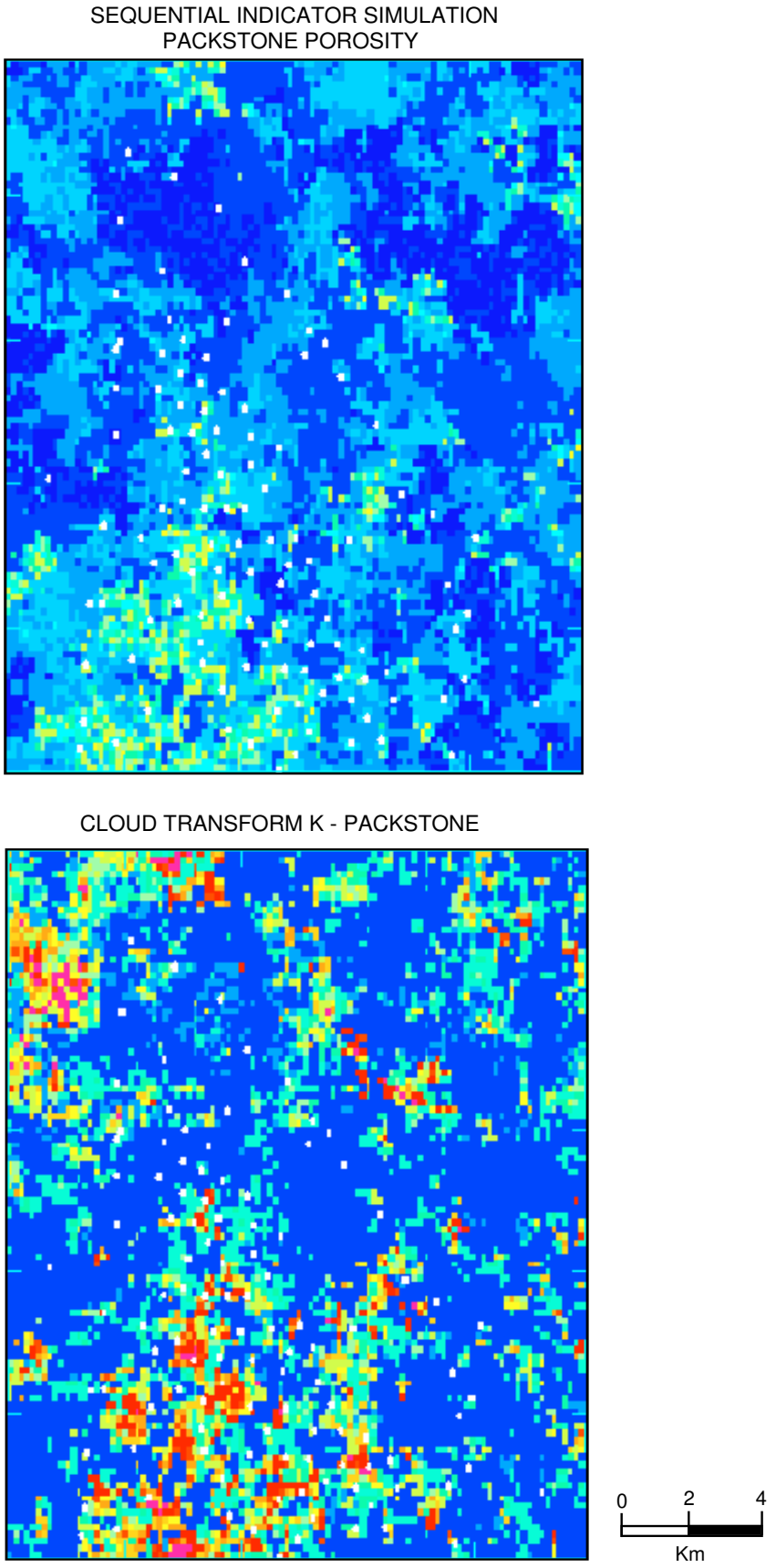

Figure 13: Comparison of an SIS porosity model for packstone electro facies and the corresponding cloud transform permeability model. Note the expected similarity of the permeability model to the porosity model.

Comparison of Model Kh to Well Test Kh

In order to further assess the usefulness of the model, comparisons of model Kh against independently obtained measures of Kh derived from engineering well tests were made. The well test data did not influence the North 'Ain Dar geostatistical permeability models; these are based exclusively on core plug data, and as such constitute matrix permeability models. The well test data was not used because of the much greater sample volume it represents; the two permeability data sets cannot be linked in modeling in a straightforward way because of scaling up concerns. The two data sets are nonetheless worth comparing to see if the patterns of distribution are similar, i.e. that both are responding in an equivalent manner to factors in the reservoir related to flow.

For comparative purposes, the well test Kh has been allocated vertically on the basis of production flowmeter log data, allowing direct comparisons to be made with model permeability. Figures 14 and 15 show comparative cumulative Kh plots for two of the wells in the pilot area for which well test data was available. It can be seen that the vertical patterns of Kh distribution are similar, that is, the inflection points in both the model and well test Kh curves occur at about the same levels. It can further be seen that the inflections occur at or near the stratigraphic markers that separate reservoir time slice intervals. In both wells, as an example, the first significant development of Kh occurs immediately below the Z-2B2 marker that separates Intervals 5 and 6 (Figures 14 and 15). Furthermore, there are marked increases in Kh contribution at or near the Z-2B1 and Z-2A1 marker surfaces. Finally, total Kh levels are comparable, though in the two examples shown (Figures 14 and 15) there is somewhat more Kh indicated by the well test data. Overall, however, the permeability populations indicated for model and well test K are in close agreement, as illustrated in Figure 16, which compares K backed out from well test Kh data with model K for a group of 31 wells. The ratio $K_{average}$*well test*/$K_{average}$*model* is 0.95 for this group of wells. The highest absolute K values are contained in the model.

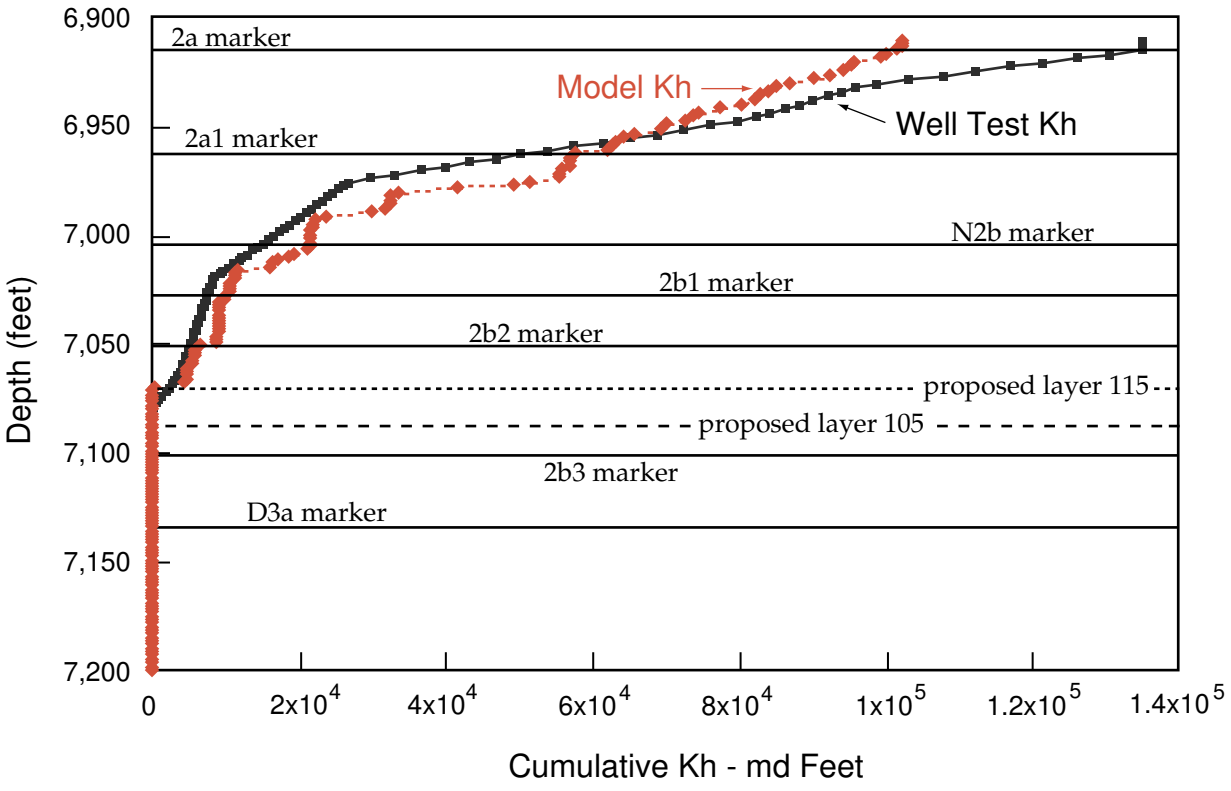

Figure 14: Comparison of model Kh to well test Kh from North 'Ain Dar well. Model Kh is shown in red and well test Kh is shown in black. The well test Kh has been allocated by reservoir engineering on the basis of flowmeter data. Note the good agreement between model-derived Kh and the actual, flowmeter-allocated Kh from the well test. Also note that Kh inflection points from the model and from the well test correspond closely to the stratigraphic markers, indicating that the porosity-gamma ray log stratigraphy is defining reservoir flow units.

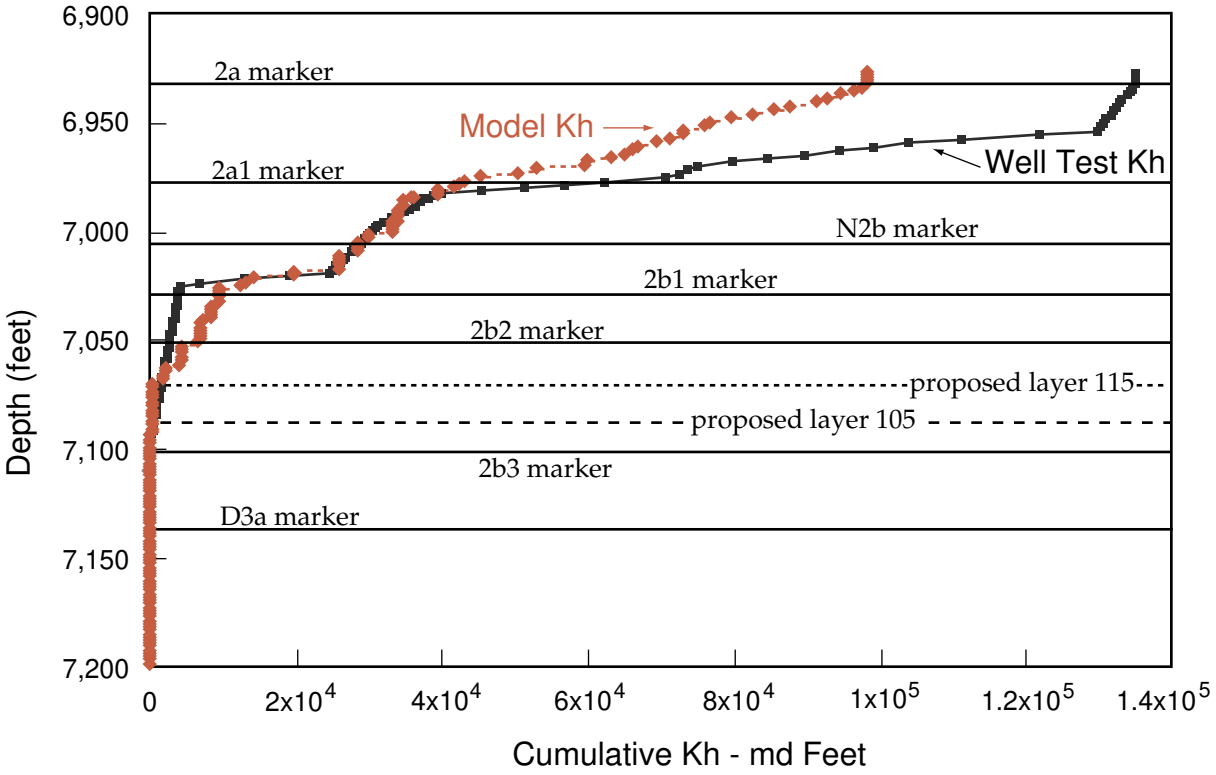

Figure 15: Comparison of model Kh to well test Kh from North 'Ain Dar well.

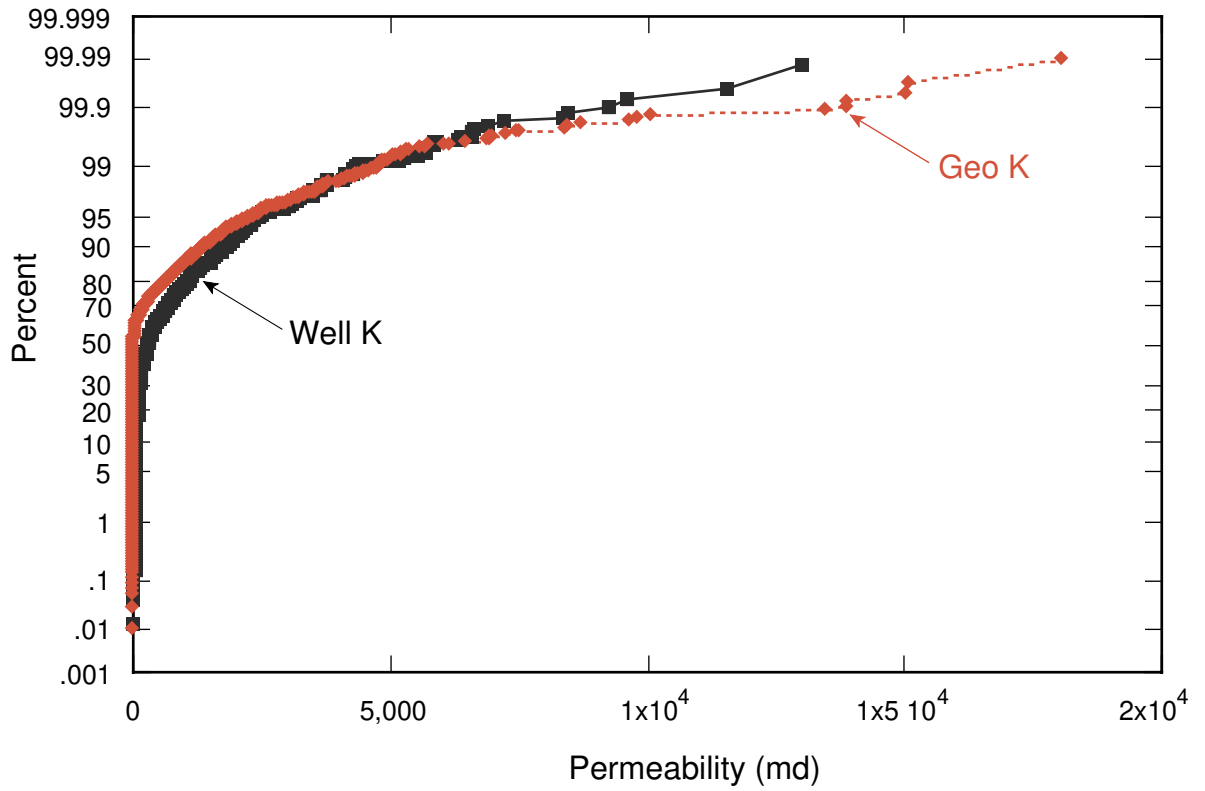

Figure 16: Global comparison of model K and well test allocated K populations for 31 well locations in the North 'Ain Dar pilot area. Note the excellent agreement between the two, with a ratio of average K_{well} to average K_{model} of 0.95. Well test K data backed out from allocated well test Kh for purposes of plot.

CONCLUSIONS

The geostatistical methods employed in constructing the North 'Ain Dar geological model are believed to have produced an improved reservoir model.

(1) Model Kh is in close agreement with well test Kh in terms of the absolute amounts of Kh contributed to the model. This represents an improvement over previous, deterministic models covering the North 'Ain Dar area, in which model permeability tended to be considerably lower than the permeability indicated by well test data.

(2) Vertical patterns of well test and model Kh are similar. Both measures are putting approximately the same proportions of total Kh into individual reservoir intervals. Furthermore, inflections or changes in Kh contribution tend to occur at or near the stratigraphic markers used to separate the reservoir into time slice intervals. This suggests that the reservoir zonation provided by the sequence stratigraphic framework is significant from a reservoir flow sense.

(3) Engineering work continues at this time on history matching the model; however, in a global sense the simulation model has been successful in capturing the irregular patterns of water movement from the flank injectors toward the crest of the structure. This is an improvement on the previous model covering the pilot area.

(4) The benefits derived from a geostatistical approach towards modeling which are believed to have contributed to the improved reservoir model include:
   (a) porosity and permeability models are constrained by the distribution of reservoir rock types that are distinct from each other in terms of the porosity and permeability population represented;
   (b) the patterns of spatial variability present in well log and core data, as determined from variogram analysis, are incorporated into the model, including portions of the model lying outside the available well control; and
   (c) data extremes for porosity and especially for permeability have been captured in the model.

ACKNOWLEDGEMENTS

The senior author would like to thank all of the members of the 'Ain Dar and Shedgum Reservoir Characterization Team (G.S. Kompanik, R.R. Davis, S.H. Al-Qahtani and I.M. Al-Goba) for their help and involvement in the building of the North 'Ain Dar geological model. Thanks are also due to R.E. Enwall, for his help in compiling and maintaining the model data base and for sharing his statistical and geostatistical expertise. The manuscript was improved based on critical reviews by Rick Davis and George Grover. Appreciation is extended to Saudi Aramco and the Ministry of Petroleum and Mineral Resources for permission to publish.

REFERENCES

Bashore, W.M., U.G. Araktingi, M. Levy and W.J. Schweller 1994. *Importance of a Geological Framework and Seismic Data Integration for Reservoir Modelling and Subsequent Fluid-Flow Predictions.* In J.M. Yarus and R.L. Chambers (Eds.), Stochastic Modeling and Geostatistics, Principals Methods and Case Studies. American Association of Petroleum Geologists, Computer Applications in Geology, no. 3, p. 159-175.

Bova, J.A. 1994. *Detailed Core Studies and Depositional Framework, Arab-D Reservoir, 'Uthmaniyah GOSP-11 Area.* Field and Reservoir Studies Report no. 136 (unpublished Saudi Aramco report).

Srivastava, M.H. 1994a. *An Overview of Stochastic Methods for Reservoir Characterization.* In J.M. Yarus and R.L. Chambers (Eds.), Stochastic Modeling and Geostatistics, Principals Methods and Case Studies, American Association of Petroleum Geologists, Computer Applications in Geology, no. 3, p. 3-16.

Srivastava, R.M. 1994b. *The Visualization of Spatial Uncertainty.* In J.M. Yarus and R.L. Chambers (Eds.), Stochastic Modeling and Geostatistics, Principals Methods and Case Studies. American Association of Petroleum Geologists, Computer Applications in Geology, no. 3, p. 339-345.

ABOUT THE AUTHOR

John L. Douglas *received a BSc degree from McGill University, Canada, and a PhD in Geology from Memorial University of Newfoundland, Canada. Between 1984 and 1991 he worked in Calgary, Alberta for the Research Laboratories of Texaco, Canada Resources, and ESSO Canada Resources. John's principal responsibility during this time was to provide geological support in the area of reservoir modeling to reservoir engineering and development geology groups. John is currently a member of the Southern Area Reservoir Geology Group of Saudi Aramco. His professional interests include reservoir description and modeling and the application of geostatistical methods to the spatial distribution of geological data.*

Paper presented at the 2nd Middle East Geosciences Conference and Exhibition, GEO'96, Bahrain, 15-17 April, 1996

Manuscript Received 15 March, 1996

Revised 24 April, 1996

Accepted 1 June 1996